N61339-92-C-0100, and the Naval Air Systems Command. The authors thank R. Thomas Galloway for helping to define the research objectives. The authors are also grateful to Brent York, Chris Weekley, and David Honaker for their help in developing the drag function modeling software.

References

[1]Kelley, H. J., "Reduced-Order Modeling in Aircraft Mission Analysis," *AIAA Journal*, Vol. 9, No. 2, 1971, pp. 349, 350.

[2]Burgin, G. H., et al., "An Adaptive Maneuvering Logic Computer Program for the Simulation of One-on-One Air-to-Air Combat, NASA CR-2582, Sept. 1975.

[3]Williams, D. H., and Wells, D. C., "Traffic Scenario Generation Technique for Piloted Simulation Studies," NASA TM-86397, April 1987.

[4]Miralles, C. T., Selmon, J., and Trujillo, S. M., "An Air Combat Simulation Model Suitable for the Evaluation of Agility and EFM," AIAA Paper 89-3311, Aug. 1989.

[5]Goodrich, K. H., and McManus, J. W., "Development of a Tactical Guidance Research and Evaluation System (TiGRES)," AIAA Paper 89-3312, Aug. 1989.

[6]Cloutier, J. R., "Multivariate, Minimum-Curvature Splines for Randomly-Space Data," AIAA Paper 91-2744, Aug. 1991.

[7]Anderson, J. D., *Introduction to Flight*, McGraw-Hill, New York, 1989.

Autonomous Spacecraft Gyro Failure Detection Based on Conservation of Angular Momentum

F. Landis Markley*
NASA Goddard Space Flight Center, Greenbelt, Maryland 20771
Kevin R. Kennedy† and John D. Nelson‡
Lockheed Missiles and Space Company, Inc., Sunnyvale, California, 94088
and
Edward W. Moy§
Lockheed Technical Operations Company, Greenbelt, Maryland, 20770

Introduction

THIS note describes a new gyro failure detection algorithm implemented onboard the Hubble Space Telescope (HST) to detect a class of potential gyro failures that would not have been recognized by pre-existing failure detection algorithms. This test is called the system momentum test, since it detects failures by monitoring the change in the system momentum calculated in the flight computer.

The HST was launched with six primary single-degree-of-freedom high-accuracy gyros for redundancy. The science pointing mode of the HST normally uses four gyros to provide gyro fault detection and improved smoothing of gyro noise, but good pointing performance (with reduced fault detection capability) is possible with three gyros.[1-3] The spacecraft is uncontrollable in this pointing mode with only two gyros, due to the unobservability of a body rate perpendicular to the input axes of both gyros, but vehicle health and safety can still be maintained with either the Zero Gyro Sunpoint safemode in the flight computer[4] or the hardware sunpoint capability using the Pointing and Safemode Electronics Assembly and the lower accuracy retrieval mode gyros.

The original fault detection logic in the HST flight computer monitored three types of gyro failures: a) disparity between measured and expected gyro counts, b) off-nominal values of hardware gyro error indicator bits, and c) measured gyro counts exceeding saturation limits. Unfortunately, these tests cannot detect a gyro failure that results in a near-zero gyro output independent of the actual spacecraft body rate when the commanded rate is also near zero. A gyro failure of this type, termed a "soft" gyro failure, could result from a failure of the rotor drive mechanism, for example. Any configuration of four gyros provides redundant information about individual vehicle axes, so a soft failure of one gyro would not have serious consequences; the three remaining gyros would allow computation of inaccurate but acceptable body rate information until one of the above tests caused the failed gyro to be autonomously removed from use. However, a soft gyro failure from a three-gyro configuration would cause an undetected increase in the vehicle angular velocity about an insensitive axis that the failed gyro would normally sense. In fact, the spacecraft attitude control system would attempt unsuccessfully to drive the output of the failed gyro to an exact zero rate, forcing the undetected rate to increase rapidly. A simulation of a soft gyro failure in the HST hardware/software interface facility verified that the existing safemode tests would not detect such a failure and that the spacecraft rate about the undetected axis would rapidly increase to a level high enough to endanger spacecraft health.

The inability of the existing gyro failure detection tests to detect a soft failure—and the threat of such a failure on the HST—led to the addition of the system momentum test. This test allows reliable and rapid detection of a soft gyro failure by checking the change in the system momentum calculated in the flight computer. In the event of such a failure, the control system response to incorrectly measured body rates causes a rapid change in computed system momentum. The system momentum test triggers a safemode entry upon detecting this change.

Simultaneous soft failures of two gyros from a four-gyro configuration is possible but improbable, since it requires a minimum of three hardware component failures in the shared clock controlling the two gyros. Although this failure mode has never occurred, simulations show that the result would be detected by the system momentum test.

System Momentum Test Algorithm

Changes in the total system momentum

$$\boldsymbol{H} = I\boldsymbol{w} + \boldsymbol{H}_{\mathrm{RW}} \tag{1}$$

are caused only by external disturbance torques such as aerodynamic drag and gravity gradient torques. In Eq. (1), I is the vehicle moment of inertia tensor, $\boldsymbol{w}$ is the vehicle angular velocity, and $\boldsymbol{H}_{\mathrm{RW}}$ is the reaction wheel angular momentum in the vehicle frame. Internal reaction wheel torques are balanced by Newton's third law so that any change in the spacecraft body angular momentum is balanced by an equal and opposite change in the momentum of the reaction wheels, resulting in zero net change in the system momentum. Since the external torques are small, the system momentum is slowly changing.

The system momentum is calculated in the flight computer for use in compensating gyroscopic torques and for momentum management. If any of the quantities entering into this computation is incorrect, the computed system momentum may change rapidly, with a rate of change much larger than the external disturbance torques. This is the basis of the system momentum test for soft gyro failures. This test estimates the net unmodeled environmental torque as

$$\boldsymbol{T}_{\mathrm{est}} = \frac{\mathrm{d}\boldsymbol{H}}{\mathrm{d}t} + \boldsymbol{w} \times \boldsymbol{H} - \boldsymbol{m} \times \boldsymbol{B} - \boldsymbol{T}_{\mathrm{gg}} \tag{2}$$

where $\boldsymbol{w} \times \boldsymbol{H}$ is the gyroscopic torque, $\boldsymbol{m} \times \boldsymbol{B}$ is the commanded magnetic torque, and $\boldsymbol{T}_{\mathrm{gg}}$ is an estimate of the gravity gradient torque. If all sensors are operating properly, the magnitude of $\boldsymbol{T}_{\mathrm{est}}$ will be on

Received Sept. 28, 1993; revision received Jan. 13, 1994; accepted for publication Feb. 5, 1994.

*Staff Engineer, Guidance and Control Branch, Code 712. Associate Fellow AIAA.

†Research Engineer Senior.

‡Group Engineer. Member AIAA.

§Staff Engineer.

the order of the unmodeled environmental torques. In the event of a soft gyro failure, incorrectly measured body rates and control law error cause a rapid change in computed system momentum, so T_{est} will be on the order of the reaction wheel control torques, which will be at least an order of magnitude larger than the environmental torques. The system momentum test compares the squared magnitude T_{est}^2 of the environmental torque estimate to a threshold that defines a soft gyro failure. If the threshold is exceeded for a database time interval, a safemode entry is initiated.

All the terms on the right side of Eq. (2) except for the time derivative of the system angular momentum were calculated in the flight computer prior to the development of the system momentum test. Gyro noise causes the derivative computation to be noisy, making it difficult to ensure that an actual failure will exceed the threshold continuously for a sufficient time interval to be detected by the system momentum test. In order to produce a smoother estimated change in system momentum, a second-order filter is used as part of the calculation of $d\boldsymbol{H}/dt$.

System Momentum Test Parameter Selection

To avoid having the system momentum test interpret another anomaly as a gyro failure, the safemode test threshold was set to a value high enough to avoid ambiguity, and the time interval for which the estimated torque is required to exceed the threshold was chosen carefully. Selection of system momentum test database parameters and verification of the system momentum test were accomplished by simulating various scenarios that influence changes in computed system momentum, such as vehicle maneuvers, solar array disturbances, gyro anomalies, and reaction wheel anomalies.[5]

Choosing the appropriate system momentum test threshold level required analytical calculations for all three-gyro combinations, to ensure that the system momentum test would detect an additional gyro failure. The minimum allowable threshold level T_{est}^2 is related to the reaction wheel torque capability in the direction of the uncontrolled axis, so the threshold value was set to 1.15 N^2-m^2 for a four-reaction-wheel configuration and to 0.32 N^2-m^2 for a three-reaction-wheel configuration. Under certain unlikely conditions, a reaction wheel tachometer failure could result in a value of T_{est}^2 in excess of these thresholds, due to an erroneous reaction wheel contribution to the system angular momentum computation. However, such extreme conditions would also trigger the existing reaction wheel momentum test, which compares the computed change in reaction wheel momentum with the value expected to result from the torque commands sent to the wheel. If the momentum change of any of the HST reaction wheels disagrees with its expected value for three consecutive 10-s periods, that reaction wheel is assumed to have failed and is removed from control. Therefore, the time interval for the system momentum test was set to 40 s to allow enough time for the reaction wheel momentum test to take action first and avert an unnecessary safemode entry.

Analysis of the system momentum derivative filter showed that an angular cut-off frequency of 0.2 rad/s and a damping ratio of 0.7 provide acceptable noise suppression while allowing soft gyro failure detection within a reasonable time.

Simulated System Momentum Test Performance

Simulation results show that the system momentum test is perceptive enough to detect a soft gyro failure from any three-gyro configuration. This type of failure produces a significant change in the momentum characterized by an immediate ramp in the value of T_{est}^2 of up to at least 1.3 N^2-m^2 over a 40-s duration. Simulations were made of all single-gyro failures from the four three-gyro subsets of the HST gyros (1, 2, 3, and 5) available at the time of the development of the system momentum test. The minimum T_{est}^2 of 1.35 N^2-m^2 was produced when gyro 3 failed from the gyro 1, 3, 5 combination, as illustrated in Fig. 1. Simulations of reaction wheel tachometer failures in a four-reaction-wheel configuration triggered neither the reaction wheel momentum test nor the system momentum test since T_{est}^2 remained under the threshold. Simulated tachometer failures in a three-reaction-wheel configuration did trigger the reaction wheel momentum test as designed.

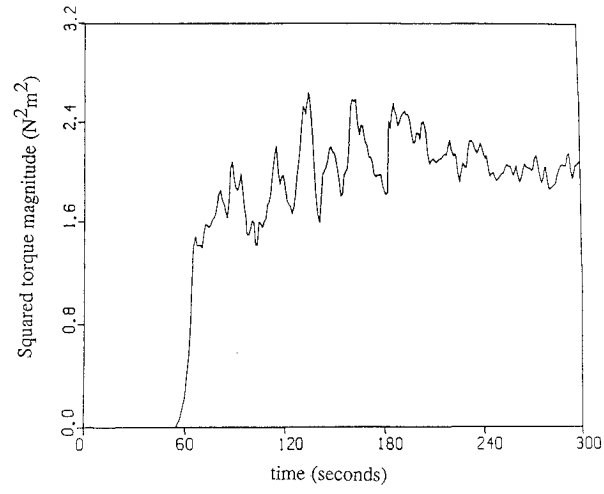

Fig. 1 Simulated environmental torque estimate squared, gyro 3 failed at 50 s.

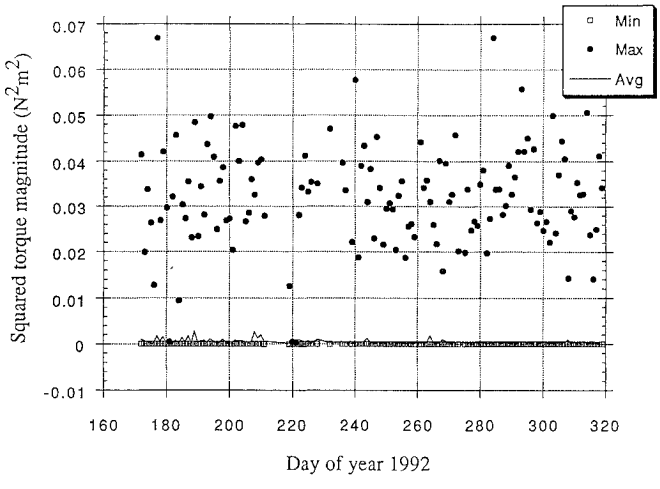

Fig. 2 Telemetered environmental torque estimate squared.

System Momentum Test Performance On-Orbit

The environmental torque magnitude has been estimated in flight since the system momentum test was uplinked on January 20/21, 1992, as part of the Zero Gyro Sunpoint safemode installation procedure.[4] Figure 2 shows the minimum, maximum, and average computed values of T_{est}^2 for 150 days in 1992. It can be seen that the maximum values consistently remained a safe amount below both the three-wheel and four-wheel threshold levels, regardless of commanded slews and spacecraft jitter caused by solar array disturbances, so the system momentum test never came close to a false indication of gyro failure.

Conclusions

The new system momentum safemode test provides reliable and rapid detection of a soft gyro failure—a failure of gyro outputs to near zero rate instead of the actual gyro rate. In the event of such a gyro failure, the control system response to incorrectly measured body rates causes a rapid change in the system momentum as calculated in the flight computer. The results of simulations for the HST show that the system momentum test is perceptive enough to detect a soft gyro failure from any three-gyro configuration. The system momentum test was uplinked to the HST on January 20/21, 1992. The test was not enabled at that time, since the HST had four functioning gyros, but its performance has been monitored in telemetry since uplink by examination of the computed environmental torque estimate. In agreement with analysis and simulation, the maximum values of this estimate have consistently remained a safe amount below the threshold level for identifying a failure, regardless of slews and solar array disturbances, so the system momentum test has never come close to a false indication of gyro failure.

Following the failure of the third of six gyros, the system momentum test was enabled on November 20, 1992. With the test enabled, a soft gyro failure in a three-gyro configuration will trigger a safemode entry to either the Zero Gyro Sunpoint safemode in the flight computer or the hardware sunpoint capability using the Pointing and Safemode Electronics Assembly along with the retrieval mode gyros. The safety provided by the system momentum test will be even more critical if the HST is routinely operated in a three-gyro configuration after the first Hubble servicing mission, as is currently planned.

Acknowledgment

We acknowledge the seminal contribution of Henry Hoffman of the Goddard Space Flight Center in insisting on the fundamental importance of angular momentum conservation.

References

[1]Dougherty, H. J., Tompetrini, K., Levinthal, J., and Nurre, G., "Space Telescope Observatory in Space," *Journal of Guidance, Control, and Dynamics*, Vol. 5, 1982, pp. 403–409.

[2]Dougherty, H. J., Rodoni, C., Rodden, J., and Tompetrini, K., "Space Telescope Pointing Control," *Astrodynamics 1983, Advances in the Astronautical Sciences*, Vols. 54 I, II, American Astronautical Society, 1983, pp. 619–630.

[3]Beals, G. A., Crum, R. C., Dougherty, H. J., Hegel, D. K., Kelley, J. L., and Rodden, J. J., "Hubble Space Telescope Precision Pointing Control System," *Journal of Guidance, Control, and Dynamics*, Vol. 11, 1988, pp. 119–123.

[4]Markley, F. L., and Nelson, J. D., "A Zero-Gyro Safemode Controller for the Hubble Space Telescope," *Journal of Guidance, Control, and Dynamics* Vol. 17, 1994, pp. 815–822.

[5]Moy, E. W., and Kennedy, K. R., "Development of System Momentum Test for Zero Gyro Sunpoint," Lockheed Missiles and Space Co., Engineering Memorandum SPS 672, Sunnyvale, CA, Feb. 1992.

Pointing Dynamics of Gimbaled Payloads on Flexible Spacecraft

Bruno Marco Quadrelli*
Georgia Institute of Technology, Atlanta, Georgia 30332
and
Andreas H. von Flotow†
Hood Technology Company, Hood River, Oregon 97031

Introduction

IMPORTANT to certain missions is to point a small, rigid instrument gimbaled to a host spacecraft using gimbal torquers as actuators. If the gimbal torquers are perfect torque actuators (free of friction, backlash, elasticity, and other real effects) and if the gimbal axis passes through the payload mass center and is parallel to a payload principal axis of inertia, then the payload pointing dynamics will be unaffected by host spacecraft dynamics. The host spacecraft will be, of course, disturbed by the gimbal torques. The more common situation has the gimbal axis neither parallel to a payload inertia axis nor passing through the payload mass center. In addition, the gimbal axis may not be aligned with any of the principal axes of the spacecraft. In this case, the payload pointing dynamics (the transfer function from gimbal torque to payload inertial attitude angle) reflect the dynamics of the host spacecraft even with perfect torque actuators. This Note offers a simple derivation for this coupling and applies it to an example. In the case of low-mass or near-CG (center of gravity)-mounted payload, we show that the payload pointing dynamics are only slightly perturbed by host spacecraft dynamics. In particular, each spacecraft flexible mode contributes one nearly canceling pole-zero pair to the payload pointing transfer function. Reference 1 has studied the use of gimbal reactuation, in which gimbal torques are reacted, not against the host spacecraft, but against a reaction wheel mounted within the gimbal. This Note shows that such reactuation can help reduce the coupling but may also strengthen it.

Received May 20, 1992; revision received Nov. 5, 1993; accepted for publication Nov. 6, 1993.

*Graduate Student, Department of Aerospace Engineering. Member AIAA.

†President. Member AIAA.

Analysis

To see how the spacecraft flexibility influences in general the pointing dynamics of an articulated body of much smaller size mounted on it, consider the general two-dimensional system depicted in Fig. 1. The payload inertial angle is θ. The gimbal torque is τ. The gimbal constraint force perpendicular to the payload reference line u is F_v, and v is the corresponding inertial displacement. The payload moment of inertia about the center of mass is J, its mass is m, and the distance to the mass center from the gimbal axis is d. Assume also that the gimbal couples the payload and the spacecraft through a one-degree-of-freedom joint and that all motion is within the plane. We derive here the relevant linear equations of motion, based upon the assumption of small perturbations away from the reference configuration. The analysis includes both flexible and rigid-body motion.

The equilibrium of torques about the payload CG gives

$$\tau - F_v d = J\ddot{\theta} \tag{1}$$

The equilibrium of forces in the v direction is

$$F_v = m(\ddot{v} + d\ddot{\theta}) \tag{2}$$

and the relevant admittance relationship for the planar response of the spacecraft, not loaded by the payload, can be written as

$$\begin{pmatrix} \ddot{v} \\ \ddot{\theta} \end{pmatrix} = \begin{bmatrix} H_{vv} & H_{v\theta} \\ H_{\theta v} & H_{\theta\theta} \end{bmatrix} \begin{pmatrix} -F_v \\ \tau \end{pmatrix} \tag{3}$$

Combining these three equations in the frequency domain, one gets the following expression for the transfer function from torque t to inertial angle q:

$$\frac{\theta(s)}{\tau(s)} = \frac{(1 + mH_{vv}) + mdH_v\theta}{J(1 + mH_{vv}) + md^2} \frac{1}{s^2} \tag{4}$$

This expression shows where the spacecraft flexibility appears and also tells us that its effect is negligible when m is very small (very light payload) or when $d = 0$ (CG-mounted payload). Basically, the difference between the flexible and rigid-body transfer functions depends on the ratio of the payload inertia to base-body inertia characteristics.

To analyze the contribution of an individual flexible mode, it is useful to expand the spacecraft admittances H_{vv} and $H_{v\theta}$ in a

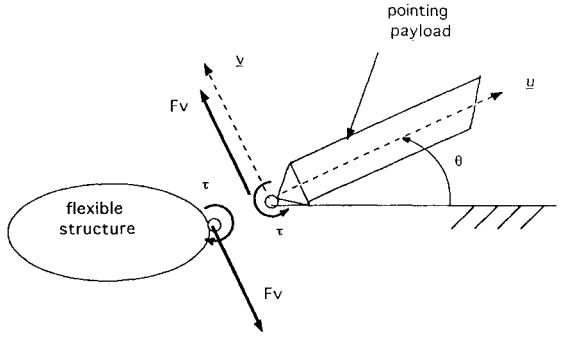

Fig. 1 Plane motion of a rigid payload gimbaled to a flexible spacecraft.